Shuttle Entry Guidance Revisited

K. D. Mease and J.P. Kremer
Department of Mechanical
and Aerospace Engineering
Princeton University
Princeton, NJ

AIAA Guidance, Navigation and Control Conference
August 10-12, 1992 / Hilton Head Island, SC

SHUTTLE ENTRY GUIDANCE REVISITED

Kenneth D. Mease* and Jean-Paul Kremer**
Department of Mechanical and Aerospace Engineering
Princeton University, Princeton, New Jersey 08544-5263

ABSTRACT

The entry guidance law for the Space Shuttle Orbiter is revisited using methods either not available or not widely used at the time the Shuttle entry guidance was developed. The feedback linearization method of differential geometric control and the nonlinear stability analysis methods of dynamical systems theory are shown to provide new perspectives on the derivation and performance of the entry guidance law. The Shuttle guidance concept is to track a reference drag trajectory that has been designed to lead to a specified range and velocity. The Shuttle guidance law provides exponential tracking locally. An approximate method of constructing the domain of attraction has been proposed and its range of validity ascertained by simulation. Using the feedback linearization method, an alternative guidance law yielding global exponential tracking, in the absence of control saturation, has been derived. For the operating domain and control capability of the Shuttle, the alternative guidance law does not improve on the stability and performance of the current guidance law. With a larger operating domain and increased lift-to-drag capability, however, the new guidance law would be superior.

NOMENCLATURE

$\dot{(\ )}$	first time derivative
$\ddot{(\ )}$	second time derivative
$(.)_0$	initial value
$(.)_f$	final value
$(.)_r$	reference value (at given V)
$\Delta(.)$	error = (.) - $(.)_r$
$\delta(.)$	linear part of $\Delta(.)$
$O(.)$	'order of operator
C_D	drag coefficient
C_L	lift coefficient
D	specific drag
e	drag error = ΔD
g	specific gravity
γ	flight path angle
g_a	apparent gravity
H	atmosphere scale height
K_d	derivative feedback gain
K_p	proportionnal feedback gain
L	specific lift
λ	eigenvalue
L_v	vertical component of $LV = L \cos\sigma$
m	vehicle mass
μ	gravitational constant
R	downrange
ρ	atmospheric density
r	radius from planet center
ρ_s	atmospheric density at r_0
r_s	planet radius
A	reference area
σ	bank angle
T	period
t	time
u	control
V	velocity
V_c	circular velocity
V_s	singularity velocity - see eq. (34)
ω	characteristic frequency
ζ	damping

* Assistant Professor
** Associate Fellow AIAA
Graduate Research Assistant
Student Member **AIAA**

INTRODUCTION

In developing guidance logic for future aerospace vehicles – an aeroassisted orbital transfer vehicle, a Mars lander, an aerospace plane, a Space Station assured crew return vehicle – one is faced with an overwhelming number of potentially applicable design approaches: neighboring optimal control, dynamic programming, neural networks, H-infinity control, regular and singular perturbation methods, adaptive control, mu-synthesis,

quantitative feedback theory, differential geometric control, dynamical systems theory, and, let us not forget, classical linear control. It is instructive in this situation to consider what approaches have been used in designing the guidance logic for current operational vehicles, why these approaches were used, and how effective they have been. Important references in this regard are [Win63,Bry68] which cover operational vehicles through Apollo. The U.S. Space Shuttle is another obvious point of focus at present.

The entry guidance for the Shuttle, in particular the logic for guiding the vehicle from atmospheric entry to the range and velocity at which the terminal area energy management phase is initiated, is the topic of this paper. The Shuttle entry guidance logic has been presented by Harpold and Graves [Har79]. The Shuttle entry guidance concept evolved from the Apollo entry guidance concept [Lic63, Mor66]. The Shuttle entry guidance has proven very effective operationally [Har83].

In this paper, the Shuttle entry guidance is revisited. The feedback linearization method of differential geometric control [Isi89] and the nonlinear stability analysis methods of dynamical systems theory [Guc83], methods which were either not available or not widely used at the time the Shuttle entry guidance was developed, are shown to provide new perspectives on the derivation and performance of the entry guidance.

The notation and assumptions for the formulation of the entry guidance problem are consistent with those in [Har79], except that several additional simplifications are made in order not to clutter the presentation of the key points. Only the longitudinal translational motion of the vehicle is considered. The aerodynamic coefficients are assumed constant. The bank angle is considered to be the only control for the translational dynamics, the angle of attack being fixed at a value dictated by heating considerations.

EQUATIONS OF MOTION

The earth-relative longitudinal translational state of the Shuttle is represented by the variables: R, r, V and γ. Neglecting the Coriolis and centrifugal terms due to the earth rotation, the equations of unpowered flight are

$$\frac{dR}{dt} = V \cos\gamma \tag{1}$$

$$\frac{dr}{dt} = V \sin\gamma \tag{2}$$

$$\frac{dV}{dt} = -D - g \sin\gamma \tag{3}$$

$$\frac{d\gamma}{dt} = \frac{1}{V}\left\{L_U - \left(g - \frac{V^2}{r}\right)\cos\gamma\right\} \tag{4}$$

The specific drag and the specific vertical lift are given by

$$D = \frac{1}{2}\rho\frac{A}{m}V^2 C_D \tag{5}$$

$$L_U = \frac{1}{2}\rho\frac{A}{m}V^2 C_L \cos\sigma \tag{6}$$

The aerodynamic coefficients C_D and C_L are assumed constant for our purposes here. An exponential atmospheric density model

$$\rho = \rho_S \exp\left(-\frac{(r - r_S)}{H}\right) \tag{7}$$

with constant density multiplier ρ_S and constant scale height H, and a constant gravitational acceleration g are assumed for the guidance law development.

The translational state is controlled by adjusting the bank angle. Equivalently, the vertical lift-to-drag ratio L_U/D is taken to be the control in the following analysis.

GUIDANCE LAW DERIVATION

The Shuttle entry guidance concept [Har79] is to choose a flyable reference trajectory that leads to the desired range at a specified velocity and to track the reference trajectory based on feedback. Following a brief discussion of the reference trajectory, we focus our attention on the tracking problem for the remainder of the paper.

Reference Drag Trajectory

Since the destination for the entry phase under consideration is a desired range at a specified velocity, it is appropriate to look at how range changes with velocity. Combining Eqs. (1) and (3), separating variables, and integrating yields

$$R(V_f) = -\int_{V_0}^{V_f} \frac{V}{D(V)}\,dV \tag{8}$$

assuming $R(V_0) = 0$ and $D >> |g \sin\gamma|$. (If the latter assumption is invalid, energy can be used in place of velocity as the independent variable.) In this light, the range is seen to depend solely on the drag versus

velocity profile. This is convenient because the entry corridor defined by structural, thermal, and controllability constraints can be represented in the drag-velocity plane. A reference trajectory $D_r(V)$ lying inside the entry corridor is selected such that the desired range is achieved at the specified velocity. The reference trajectory for the Shuttle entry is a continuous spline of two quadratic segments, a pseudo-equilibrium glide segment, a constant drag segment, and a linear energy segment. The reference trajectory is biased toward the higher drag side of the entry corridor to reduce the total heat load by reducing the flight time to the specified velocity.

Reference Trajectory Tracking

Once the reference drag versus velocity trajectory is chosen, it remains to develop the bank angle control law for tracking the reference trajectory. The drag is the focus of attention, so we think of it as the output of the third-order dynamical system given by Eqs. (2) – (4). (The range equation is neglected since the dynamical system that generates the drag does not depend on the range.) The approach to deriving the bank angle control law begins with time differentiating the drag along a trajectory (i.e., taking the Lie derivative of the drag) until the first appearance of the control. The first and second derivatives are

$$\dot{D} = -\frac{DV}{H}\sin\gamma - \frac{2D^2}{V} \tag{9}$$

$$\ddot{D} = a(V, D, \dot{D}) + b(V, D, \dot{D})\,u \tag{10}$$

where

$$a = \dot{D}\left(\frac{\dot{D}}{D} - \frac{3D}{V}\right) - \frac{4D^3}{V^2} + \left(\frac{D}{H}\right)\left(g - \frac{V^2}{r}\right)$$

$$b = -D^2/H$$

$$u = L_U/D$$

Eqs. (9) and (10) have been derived under the assumptions that $D >> |g \sin\gamma|$ and $\cos\gamma = 1$. Eqs. (9) and (10) have singularities at $V=0$ and $D=0$. Given the velocity range of interest and the assumptions employed in deriving Eqs. (9) and (10), we have already confined our attention to the domain defined by $V > 0$ and $D > 0$; the singularities will not be encountered. We further assume that r in the apparent gravity term $(g - V^2/r)$ is constant to simplify the subsequent developments.

We set as our goal to construct a control law that yields asymptotic tracking of the reference trajectory when the models given above are exact and the fedback state variables are measured without error. It is also necessary that the transient response is sufficiently fast. It is the reference drag versus velocity trajectory that leads to the desired range at the specified velocity; if the control law does not cause quick enough recovery from perturbations off the reference trajectory, the desired final condition will not be achieved.

Let

$$\nu = a(V, D, \dot{D}) + b(V, D, \dot{D})\,u(V, D, \dot{D}) \tag{11}$$

and consider u to be a function of the arguments shown. Defining $\Delta a = a - a_r$, $\Delta b = b - b_r$ and $\Delta u = u - u_r$, where $a_r = a(V, D_r, D_r)$ and similarly for b_r and u_r, Eq. (11) is rewritten as

$$\begin{aligned}\nu &= (a_r + b_r\,u_r) + (\Delta a + \Delta b\,u_r + b\,\Delta u)\\ &= \nu_r + \Delta\nu\end{aligned} \tag{12}$$

where ν_r and $\Delta\nu$ correspond to the first and second expressions in parentheses, respectively, and $\Delta\nu(V, D_r, D_r) = 0$. Eq. (10) becomes

$$\ddot{D} = \nu_r + \Delta\nu \tag{13}$$

Choosing

$$\nu_r = \ddot{D}_r \tag{14}$$

and defining $\Delta D = D - D_r$, the dynamics for the tracking error are given by

$$\Delta\ddot{D} = \Delta\nu \tag{15}$$

The feedforward control

$$u_r = \frac{1}{b_r}(-a_r + \ddot{D}_r) \tag{16}$$

thus produces perfect tracking beyond any value of V for which ΔD and $\Delta\dot{D}$ are both zero. (Note that $b_r \neq 0$, since $D > 0$.) However, if only the feedforward control is used (i.e., $\Delta u = 0$), the resulting time-varying error dynamics are

$$\Delta\ddot{D} = \Delta a + \Delta b\,u_r \tag{17}$$

which may not be acceptable. The simplest acceptable error dynamics are of the linear, time-invariant form

$$\Delta\ddot{D} + 2\zeta\omega\,\Delta\dot{D} + \omega^2\,\Delta D = 0 \tag{18}$$

with positive natural frequency ω and positive damping ratio ζ, since the error dynamics are then asymptotically (or, more precisely, exponentially) stable with respect to the origin.

Controllability and Performance Subsets of Error State Plane

It is important for subsequent developments to define two closed subsets of the error state plane. We use e and $\dot{e}$ interchangably with ΔD and $\Delta\dot{D}$ for the error state variables. The first we call the controllability subset C_2 defined by

$$C_2(V, (L_v/D)_{max}) = \{(e, \dot{e}): e_{min} \le e \le e_{max}$$

$$and\ \dot{e}_{min} \le \dot{e} \le \dot{e}_{max}\}$$

where $e_{min} < 0$ and $e_{max} > 0$ depend on V, e, and $(L_v/D)_{max}$, and $\dot{e}_{min} < 0$ and $\dot{e}_{max} < 0$, respectively. For simplicity, the bounds on $\dot{e}$ are assumed to be independent of V; they are determined by the constraints and reference drag trajectory via Fig. 1 and perhaps other considerations. We shall not be more specific than this. The error rate bounds ensure that there is sufficient control capability to keep the error within its bounds, As $(L_v/D)_{max} \to \infty$, $\dot{e}_{min} \to -\infty$ and $\dot{e}_{max} \to \infty$.

The performance subset P_2 is defined by

$$P_2(V, \zeta, \omega) = \{(e, \dot{e}): e_{min} \le e \le e_{max}$$

$$and\ \dot{e}_l(e) \le \dot{e} \le \dot{e}_u(e)\}$$

P_2 differs from C_2 only in the error rate bounds. P_2 is the set of points in the error state plane at a given V that do not violate the error bounds when propogated forward in time according to the specified error dynamics in Eq. (18). The lower and upper error rate bounds $\dot{e}_l$ and $\dot{e}_u$ depend on V, e, ζ, ω, and the error bounds, and are the graphs of the state plane trajectory segments corresponding to Eq. (18).

By taking the union of $C_2(V)$ over the range of V of interest, we obtain the controllability set C_3 for the three-dimensional $(e, \dot{e}, V)$ space. We compose P_3 similarly. It is only reasonable to require the target error dynamics given in Eq. (18) to be achieved on the intersection of C_3 and P_3, the task being impossible otherwise.

Local Asymptotic Tracking

The approach taken in the derivation of the Shuttle guidance was to specify a linear feedback control u such that the tracking error dynamics given in Eq. (18) are achieved locally. Thus consider A_U to be linear in D and $\dot{D}$

$$A_U = -K_p(V)\,\Delta D - K_d(V)\,\Delta\dot{D} \tag{19}$$

and consider the linear part of the expansion of Δv about the reference drag trajectory for fixed V

$$\delta v = \left(\frac{\partial a}{\partial D} + u_r\frac{\partial b}{\partial D}\right)\Delta D + \left(\frac{\partial a}{\partial \dot{D}} + u_r\frac{\partial b}{\partial \dot{D}}\right)\Delta\dot{D} + b_r\,\Delta u \tag{20}$$

where all the partial derivatives are evaluated on the reference trajectory. The closed-loop linear variational equation is

$$\Delta\ddot{D} + \left(b_r K_d - \frac{\partial a}{\partial \dot{D}} - u_r\frac{\partial b}{\partial \dot{D}}\right)\Delta\dot{D} + \left(b_r K_p - \frac{\partial a}{\partial D} - u_r\frac{\partial b}{\partial D}\right)\Delta D = 0 \tag{21}$$

The desired asymptotically stable error dynamics are achieved locally by specifying the gains

$$K_p = \frac{1}{b_r}\left(\omega^2 + \left(\frac{\partial a}{\partial D}\right)_r + u_r\left(\frac{\partial b}{\partial D}\right)_r\right) \tag{22}$$

$$K_d = \frac{1}{b_r}\left(2\zeta\omega + \left(\frac{\partial a}{\partial \dot{D}}\right)_r + u_r\left(\frac{\partial b}{\partial \dot{D}}\right)_r\right) \tag{23}$$

which are automatically scheduled on V (note that the partial derivatives vary with V) to give the desired constant coefficient closed-loop dynamics. The complete control law used for the Shuttle entry is

$$u = \frac{1}{b_r}\left(-a_r + \ddot{D}_r\right) - K_p(V)\,\Delta D - K_d(V)\,\Delta\dot{D} \quad (24)$$

In the Shuttle entry guidance, there are additional features which are neglected here because they deal with aspects of the guidance problem we are not considering. Altitude rate is fed back in place of drag rate, since it can be determined with less error. There is an integral term in addition to the proportional and derivative terms in the control law for the obvious reasons. And, there is the capability of recomputing the reference drag trajectory during the entry, although it has not been important for the Shuttle flights to date.

Feedback Linearization Method

In the formalism of the feedback linearization method [Isi89], we have used a nonlinear state transformation and a state-dependent control transformation to linearize the input-output dynamics. The state variables (r, γ, V) were transformed to $(D, \dot{D}, VI$ and the control was transformed according to **Eq. (11).** Using the notation $(z_1, z_2, z_3) = (D,$ D, $VI,$ the transformed state equations are

$$z_1 = z_2 \quad (25)$$

$$z_2 = \mathrm{v} \quad (26)$$

$$\dot{z}_3 = -z_1 + gH\left(\frac{z_2 z_3 + 2z_1^2}{z_1 z_3^2}\right) \quad (27)$$

$$Y = z_1 \quad (28)$$

and the state space is defined as $S = \{(z_1, z_2, z_3): z_1 > 0$ and $z_3 > 0\}$. This definition of the state space excludes the $D = 0$ plane on which the inverse state and control transformations are not well-defined and the unphysical negative drag and negative velocity regions. The dynamical system between input v and output y is linear, time-invariant and in double-integrator form. Because the control first appeared in the second Lie derivative of the output, the system given by Eqs. (1)-(3) and the output D is of relative degree two. The behavior of the third state variable z_3 is not observable in the output.

Note that by specifying

$$\mathrm{v} = a + b\,u = \ddot{D}_r - \omega^2\,\Delta D - 2\zeta\omega\,\Delta\dot{D} \quad (29)$$

the target error dynamics given in **Eq.** (18) are achieved *globally* on $C_2 \cap P_2$ for each value of V in the range of interest. The required actual control is

$$u = \frac{1}{b}\left(-a + \ddot{D}_r - \omega^2\,\Delta D - 2\zeta\omega\,\Delta\dot{D}\right) \quad (30)$$

which is well-defined on S. This global asymptotic tracking control law is *nonlinear* due to the dependence of a and b on D and D. By expanding the control law about D_r and $\dot{D}_r$ at each value of V to obtain the form

$$u = u_r + \delta u + O(\delta u^2) \quad (31)$$

it can be shown that the Shuttle law in Eq. (24) is obtained by neglecting the second and higher order terms. Fig. **2** shows the block diagram for the closed-loop system.

When the relative degree, two in our case, is less than the dimension of the internal state, three in our case, some of the behavior of the system is not observable in the output, and there is concern as to the nature of this behavior. For the tracking problem, the tracking error, $AD = D - D_r = z_1 - D_r$, may be thought of as the output of interest. Perfect tracking implies that z_1 and z_2 are behaving as desired, but implies nothing about the behavior of **23.** Thus in general one must analyze the dynamics of z_3 when the tracking error output is zero, referred to as the *zerodynamics,* to determine if they are acceptable. Geometrically, the perfect tracking conditions $AD \equiv 0$ and $\dot{AD} \equiv 0$ define a one-dimensional manifold in the three-dimensional state space and the zerodynamics dictate the motion on this manifold. For gliding (unpowered) entry and a reference drag trajectory within the corridor as shown in Fig. **1,** the velocity, z_3, is strictly monotonically decreasing along the reference drag trajectory, and presents no cause for concern.

In general, in using the feedback linearization method, one must also be concerned that, although the behavior of the observable part of the transformed state is acceptable, the behavior of the original variables may not be. This is not a concern here because the transformed variables are the variables of interest; they are physical variables, the variables in which the important constraints are expressed.

Another important issue is control saturation. Both the linear (Shuttle) and nonlinear tracking laws are obtained by specifying desired closed-loop error dynamics and then obtaining the required control by an inversion process. The vertical lift-to-drag ratio has been designated as the control in the above formulation. For a given vehicle at a fixed

angle of attack, there is a maximum positive and maximum negative vertical lift-to-drag ratio; any value of L_v/D between and including these extremes can be achieved by an appropriate bank angle. If the L_v/D commanded by the tracking law is outside of the achievable range, there is saturation and the closed-loop dynamics will not be as desired. Given that there will be control saturation, the nonlinear law may not yield global asymptotic tracking on $C3 \cap P3$; if it does, the performance may not conform to the target dynamics in Eq. (18).

GLOBAL STABILITY AND PERFORMANCE

In this section, the global behavior of the closed-loop tracking system in the error state plane is analyzed for the linear and the nonlinear control laws, with unbounded and bounded control. Given the extensive testing of the Shuttle guidance logic and the operational success, the domain of attraction will surely be adequate for the Shuttle parameters. Our interest is in how the domain of attraction varies with control and other parameters and, for initial errors within the domain of convergence, how the performance of the linear tracking law compares to that of the nonlinear tracking law.

Stability with Unbounded Control

In the absence of control saturation, the global closed-loop tracking error behavior for the nonlinear tracking law obtained by the feedback linearization method is clear, since the error dynamics are globally linear and independent of V. There is a unique aymptotically stable equilibrium point at the origin, and the domain of attraction for this equilibrium point is the entire plane, i.e., the origin is globally asymptotically stable.

The global closed-loop tracking error behavior for the Shuttle tracking law, on the other hand, is more difficult to determine. The error dynamics are of the form

$$\Delta\ddot{D} = -2\zeta\omega\,\Delta\dot{D} - \omega^2\,\Delta D + h(\Delta D,\ \mathrm{AD},\ V) \qquad (32)$$

where $h(\Delta D,\ \mathrm{AD}, V)$ contains second and higher order terms in the drag error and its derivative. In the neighborhood of the origin where $h(\Delta D,\ \Delta\dot{D}, V)$ is negligible, the behavior is independent of V and identical to that for the nonlinear tracking law, provided the same values of ζ and ω are used. The origin is an aymptotically stable equilibrium point. Outside the neighborhood of the origin, however, the nonlinear terms in the error dynamics become important and the behavior for Shuttle law differs from that for the nonlinear law. The analysis of the global behavior for the Shuttle law is not straightforward, because the nonlinear terms in the error dynamics depend explicitly on V. One approach is based on a time-scale separation argument.

A working hypothesis is that the error dynamics evolve on a faster time-scale than the velocity dynamics, and thus the V-dependent tracking error behavior can be analyzed by patching together the error state portraits (i.e., phase portraits [Guc83]) for fixed values of V. In the (AD, $\dot{\mathrm{A}}\mathrm{D}$, V) space, the zero tracking error trajectory lies along the Vaxis. Our interest is in determining the set of points in the three dimensional space that are attracted to the zero tracking error trajectory, i.e., the domain of attraction of the zero tracking error trajectory. The error state plane for each value of Vcontains a slice of the domain of attraction. *An* approximation of the slice is obtained by considering V as a constant parameter in the error dynamics and computing the domain of attraction for the origin in the error state plane. Patching together the slices, an approximation of the three-dimensional domain of attraction is obtained. There is precedent for this approach. For a linear system with time-varying coefficients, there is a theorem that states roughly that, **if** the coefficients are bounded with time and their rates of change are sufficiently small, then the origin is asymptotically stable, if the eigenvalues of the frozen-time system have negative real parts for all times [Bro70, Kok86]. Our hypothesis is a natural but unproven extension of this theorem. In the following, we consider the tracking of a constant drag reference trajectory in order to simplify the presentation.

For a constant drag reference trajectory, the frozen-V error dynamics with the linear control law have two equilibrium solutions. Besides the primary asymptotically stable equilibrium at the origin, there is a secondary equilibrium E2 at $(e, \dot{e}) = (\Delta D_{E2}(V),\ 0)$ where

$$\frac{\Delta D_{E2}}{Dr} = -\left(1 - \frac{g}{\mathrm{H}\,\omega^2}\left(1 - V^2/V_c{}^2\right)\right)^{-1}$$

$$= -\frac{1}{\left(1 - (g_a/\mathrm{H}\,\omega^2)\right)} \qquad (33)$$

where $g_a = g(1 - V^2/V_c{}^2)$. The secondary equilibrium lies in the V-slice of the state space S only if $\Delta D_{E2}/D_r > -1$. The inequality is satisfied for $V > V_c$ and, if $V_s > 0$ exists, for $0 < V < V_s$. V_s is defined as the nonzero velocity at which the singularity in Eq.

(33) occurs; it is the positive real solution to the equation

$$V^2 = V_c^2 (1 - \omega^2 H/g) \qquad (34)$$

Obviously, $(1 - \omega^2 H/g) > 0$ is necessary and sufficient for V_s to exist. In terms of $T = 2\pi/\omega$, the condition is $T^2 > 4\pi^2 H/g$. We note that $V_s \to V_c$ as $T \to \infty$. For a given gravity field and atmosphere, characterized by g and H, the location of the secondary equilibrium depends on the ratio of the velocity to the circular velocity V/V_c, the reference drag D_r, and the control parameter ω, or equivalently T. Fig. 3 shows the dependence of $\Delta\dot{D}_{E2}/D_r$ on V/V_c and T for the values H = 7.25 km and $g = \mu/r^2 = (3.986\ 10^5\ km^3/s^2)/(6440\ km)^2$. For these values of V and H, V_s exists for T > 172.5 s.

The eigenvalues of the stability matrix at the secondary equilibrium are the roots λ_1 and λ_2 of the characteristic equation

$$\lambda^2 + \frac{2\zeta\omega(g_a/H\omega^2)^2 - 3(g_a/H\omega^2)D_r/V}{(1 - (g_a/H\omega^2))^2}\lambda + \frac{\omega^2(g_a/H\omega^2)}{(1 - (g_a/H\omega^2))} = 0 \qquad (35)$$

At supercircular velocity, $g_a < 0$. It follows that the "constant" term in the quadratic, which is equal to the product of the eigenvalues is negative, i.e., $\lambda_1 \lambda_2 < 0$; thus, the eigenvalues are real and of opposite sign, and $E2$ is a saddle. It can be shown similarly that for $V < V_s$, when V_s exists, $E2$ is also a saddle. For the velocity range $V_s < V < V_c$, or $0 < V < V_c$ if V_s does not exist, $E2$ is asymptotically stable for the parameter values studied here. However, over this velocity range, the secondary equilibrium is not in the state space S under consideration.

The secondary equilibrium is only of interest when it plays a role in defining the basin of attraction of the primary equilibrium at the origin. The conclusion of the previous paragraph was that at velocities for which $E2$ lies in S, $E2$ is always a saddle. The stable invariant manifold [Guc83] of the saddle defines the basin of attraction for the primary equilibrium. The stable invariant manifold is computed by numerically integrating the frozen-V error dynamics backward in time form an initial condition that is a small perturbation from $E2$ in the stable eigendirection. At velocities for which $E2$ is an attractor located outside of S, numerical simulations indicate that the primary equilibrium is globally attractive within S.

The validity of our approximate method of constructing the three-dimensional basin of attraction in the $(\Delta D, \Delta\dot{D}, V)$ space is supported by the computations shown in Fig. 4. The tracking of a constant drag trajectory with D_r = 9 m/sec^2 is considered. The linear control law parameters are ζ = 0.7 and T = $2\pi/\omega$ = 500 sec. The invariant manifolds of the secondary equilibrium for V = 4.0 km/s and V = 2.5 km/s are superimposed on the error plane in Fig. 4. The stable invariant manifolds constitute the basin boundaries respectively for V = 4.0 km/s and V = 2.5 km/s; according to the hypothesis, the two basins of attraction are slices for the given values of V of the three-dimensional basin of attraction in the $(\Delta D, \Delta\dot{D}, V)$ space. Also shown in Fig. 4 are the trajectories of the varying-V error dynamics. If the boundary of the three-dimensional basin of attraction is accurately approximated by the stable invariant manifolds of the secondary equilibrium in the frozen-V error planes, trajectories originating from points within the boundary should be attracted to the origin of the error plane, and trajectories originating from points outside the boundary should not. The initial conditions are all chosen in the error plane at V = 4.0 km/s. The aerodynamic coefficients are assumed to be $C_D = C_L$ = 0.8 and the surface-to-mass ratio A/m = 0.0025 m^2/kg. The behavior of the corresponding trajectories is correctly predicted.

For values of T high enough that V_s exists, the frozen-V approximation loses its validity for velocities just under V_s. As seen in Fig. 3, the location of the secondary equilibrium changes rapidly with V near V_s. Simulations show that trajectories emanating from points within the frozen-V basin of attraction at an initial velocity near V_s may not be attracted to the reference trajectory. For velocities near V_s, the three-dimensional basin of attraction must be constructed by numerical simulation. A similar situation exists for velocities just above circular.

The location of the secondary saddle-type equilibrium and the associated stable eigendirection, and therefore, the basin of attraction in a frozen-V error plane, depend on D_r and T as well as V. (There is also a dependence on ζ, but it is not considered here.) Fig. 5a for V = 4 km/s and D_r = 9 m/s^2 and Fig. 5b for V = 10 km/s and D_r = 4 m/s^2 show the basin boundaries for several values of the control law parameter T. The Shuttle operates with T in the range 90-200 s. In this range, the domain of attraction includes all of S for V = 4 km/s and all but the lower left corner for V = 10 km/s.

Stability with Bounded Control

We now consider the effect of a realistic control bound on tracking performance and stability for both the linear (Shuttle) and nonlinear control laws. The control constraint has the form

$$| (L/D)_U | \leq [(L/D)_U]_{max} \quad (36)$$

The reference drag trajectory must not only be flyable with the available control capability, but also reserve sufficient control effort for recovery from perturbations, Accounting for control saturation alters the error dynamics for both the linear and nonlinear control laws, We consider the control bound $[(L/D)_U]_{max} = 1.0$ which is roughly the maximum hypersonic L/D for the Shuttle.

Fig. 6 shows the saturation boundaries in the error plane for the linear and nonlinear control laws for the conditions T = 200 s, a reference drag of 7 m/s^2, V= 7.8 km/s and an altitude of 60 km. The frozen-V error dynamics are affected in the following manner. For the linear law, control saturation changes the location of the secondary equilibrium ***E2,*** if E2 for the unbounded case lies in the saturated region. When *E2* is a saddle, the shape of the stable invariant manifold, and therefore the boundary of the basin of attraction, changes if the stable manifold for the unbounded case passes through the saturated region. For the nonlinear law, we find that the origin remains globally attracting for error states lying within $C_3 \cap P_3$. For both the linear and nonlinear laws, additional equilibria corresponding to the constant-control dynamics can appear in the saturated regions. In some cases, these new equilibria appear to attract the trajectories, but they are located well outside C3 n *P3* and hence have little practical importance.

Performance

In addition to stability, the transient performance of the linear and nonlinear tracking laws is of interest. The drag error dynamics have been specified to be linear second-order with prescribed period T and damping ratio ζ.

For the nonlinear tracking law and unbounded control, the guidance law derivation guarantees perfect performance within the assumptions $D >> |g \sin\gamma|$ and cosy = 1. With bounded control, the drag error behavior will depart from the specified performance when control saturation is experienced.

For the linear tracking law, the prescribed performance will be met in the neighborhood of the origin; outside the neighborhood of the origin the $h(\Delta D, AD, V)$ term in **Eq.** (32) will alter the performance from that specified. Degraded performance is particularly anticipated close to the boundary of the basin of attraction or in regions of the error plane where the linear and nonlinear laws depart significantly from each other. Control saturation is another source of performance degradation.

Fig. 7 shows an example of the performance difference between the linear and nonlinear laws and the effect of control saturation. The conditions are the same as those given for Fig. ***6,*** and the trajectories plotted in Fig. 7 are the time histories corresponding to the error state plane trajectories shown in Fig. 6. There is an initial drag rate error corresponding to a +1.52° perturbation in the flight-path angle at a velocity of **7.8** km/s. By the end **of** the trajectories, the velocity has decreased to **5.0** km/s. The solid curve in Figs. 6 and 7 is the closed-loop response with the nonlinear tracking law and unbounded control; the transient response is exactly as specified. **As** seen in Fig. 6, lift-to-drag ratios below the lower bound of **– 1** (about **– 1.5** maximum) are required to achieve the specified transient response. Taking into account the saturation, the trajectory is altered upon entering the saturated region; the dashed curve is the closed-loop response with the nonlinear tracking law and bounded control. The undershoot is increased and the response time is increased by control saturation. The dot-dashed curve is the closed-loop response with the linear tracking law and bounded control. Because the linear control is only saturated for a short time at the beginning, the unbounded and bounded responses to this initial error are not very different. Relative to the case of the nonlinear law with bounded control, the response time with the linear control law is increased and secondary overshoot develops. This degradation in the performance of the linear law is due to the neglected nonlinear error dynamics.

Implications **for** the Shuttle

The Shuttle entry guidance has of course been thoroughly validated by simulation and has proven very effective operationally [Har83]. The objective here is to gain additional insight into why the guidance law is successful, some perspective on its range of applicability, and an understanding **of** the conditions under which the alternative guidance law developed in this paper would be superior. The preceding stability and performance analysis considered only constant drag reference trajectory tracking. The actual reference trajectory tracked by the Shuttle, shown in Fig. **1,** varies with V. However, since the rate of change of D_r is relatively slow (estimated less than 0.02 m/s^3), it is not expected that the results we have obtained would be significantly

different if the variation in D_r was taken into account.

Our analysis shows as expected that the Shuttle guidance law provides exponential tracking of the reference drag trajectory within the Shuttle operating domain. The alternative nonlinear guidance law would only offer improvement if the operating domain $C_3 \cap P_3$ were expanded. If controllability is limiting the operating domain, however, the superiority of the nonlinear law would be diminished by control saturation.

CONCLUSIONS

The Shuttle entry guidance concept is to track a reference drag trajectory that leads to the specified range and velocity for the initiation of the terminal energy management phase. The current guidance law provides exponential tracking locally. An approximate method of constructing the domain of attraction has been proposed and its range of validity ascertained by simulation. Using the feedback linearization method, an alternative guidance law yielding global exponential tracking, in the absence of control saturation, has been derived. For the operating domain and control capability of the Shuttle, the alternative guidance law does not improve on the stability and performance of the current guidance law. With a larger operating domain and increased lift-to-drag capability, however, the new guidance law would be superior.

ACKNOWLEDGMENT

This research was supported by the NASA Langley Research Center under Grant NAG1-907.

REFERENCES

[Bro70] Brockett, R. W., Finite Dimensional Linear Systems, Wiley, New York, 1970.

[Bry68] Bryson, A. E., Jr., et al, Guidance and Navigation for Entry Vehicles, NASA SP-8015, Nov. 1968.

[Guc83] Guckenheimer, J. and Holmes, P., Nonlinear Oscillations. Dynamical Systems, and Bifurcations of Vector Fields, Springer-Verlag,New York, 1983.

[Har79] Harpold, J. C. and Graves, C. A., Jr., Shuttle Entry Guidance, Journal of the Astronautical Sciences, vol. 27, no. 3, pp. 239-268, July-September 1979.

[Har83] Harpold, J. C. and Gavert, D. E., Space Shuttle Entry Guidance Performance Results, J. Guidance, Control, and Dynamics, Vol. 6, No. 6, pp. 442-447, Nov.-Dec. 1983.

[Isi89] Isidori, A., Nonlinear Control Systems, second edition, Springer-Verlag, 1989.

[Kok86] Kokotovic, P. V., Khalil, H. K. and O'Reilly, J., Singular Perturbation Methods in Control: Analysis and Design, Academic Press, 1986.

[Lic63] Lickly, D. J., Morth, H. R. and Crawford, B. S., Apollo Reentry Guidance, MIT Instrumentation Laboratory Rept. R-415, 1963.

[Mor661 Morth, H. R., Reentry Guidance for Apollo, MIT Instrumentation Laboratory Rept. R-532. Vol. I, Jan. 1966.

[Win63] Wingrove, R. C., Survey of Atmosphere Re-Entry Guidance and Control Methods, AIAA Journal, vol. 1, nr 9, pp. 2019-2029, September 1963.

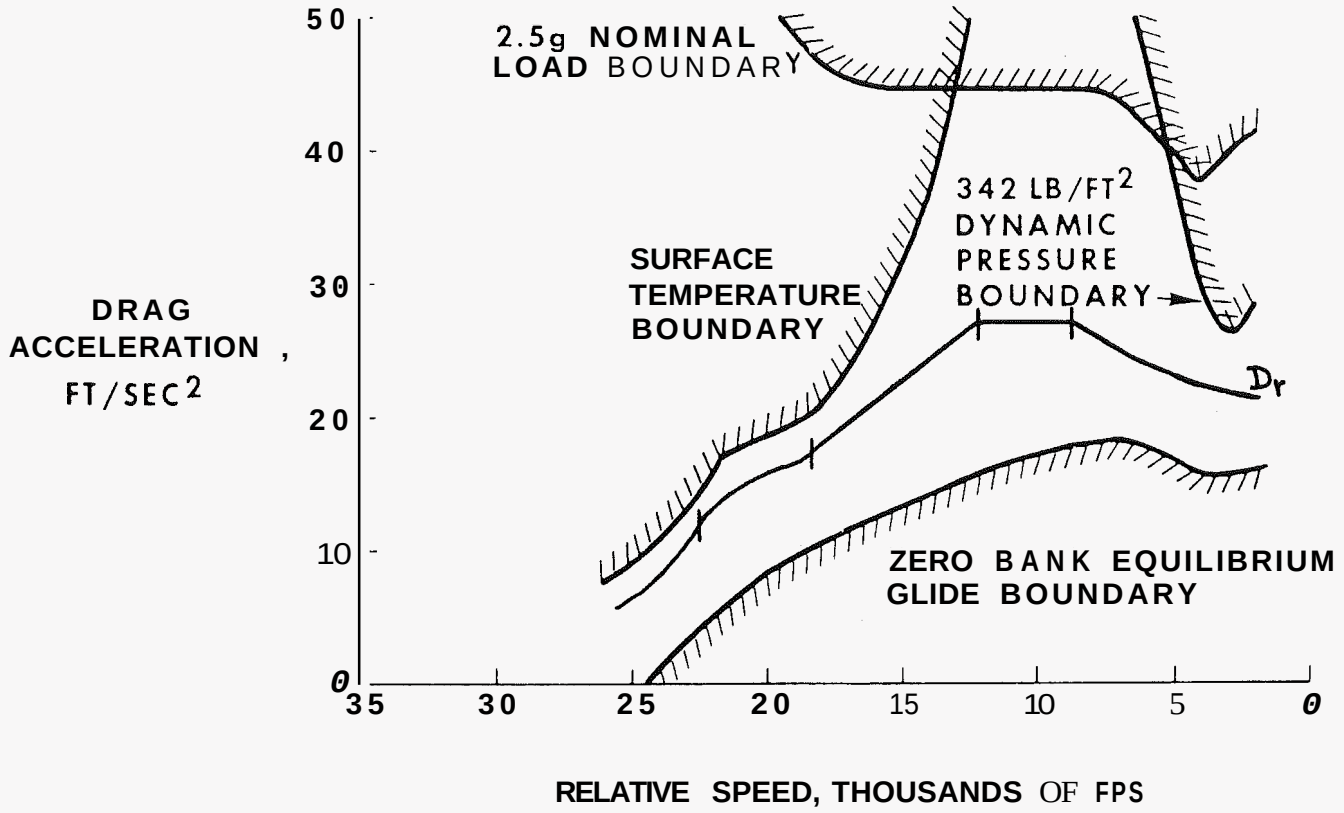

Figure 1: Operational Entry Corridor and Reference Drag Profile (Taken from [Har79])

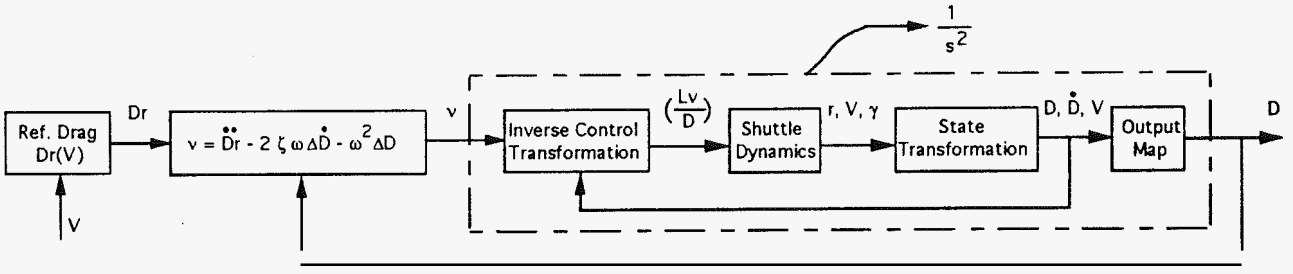

Figure 2: Block Diagram of Feedback Linearized System Subject to Feedforward and Linear Feedback Control

Fig. 3: Bifurcation Diagram

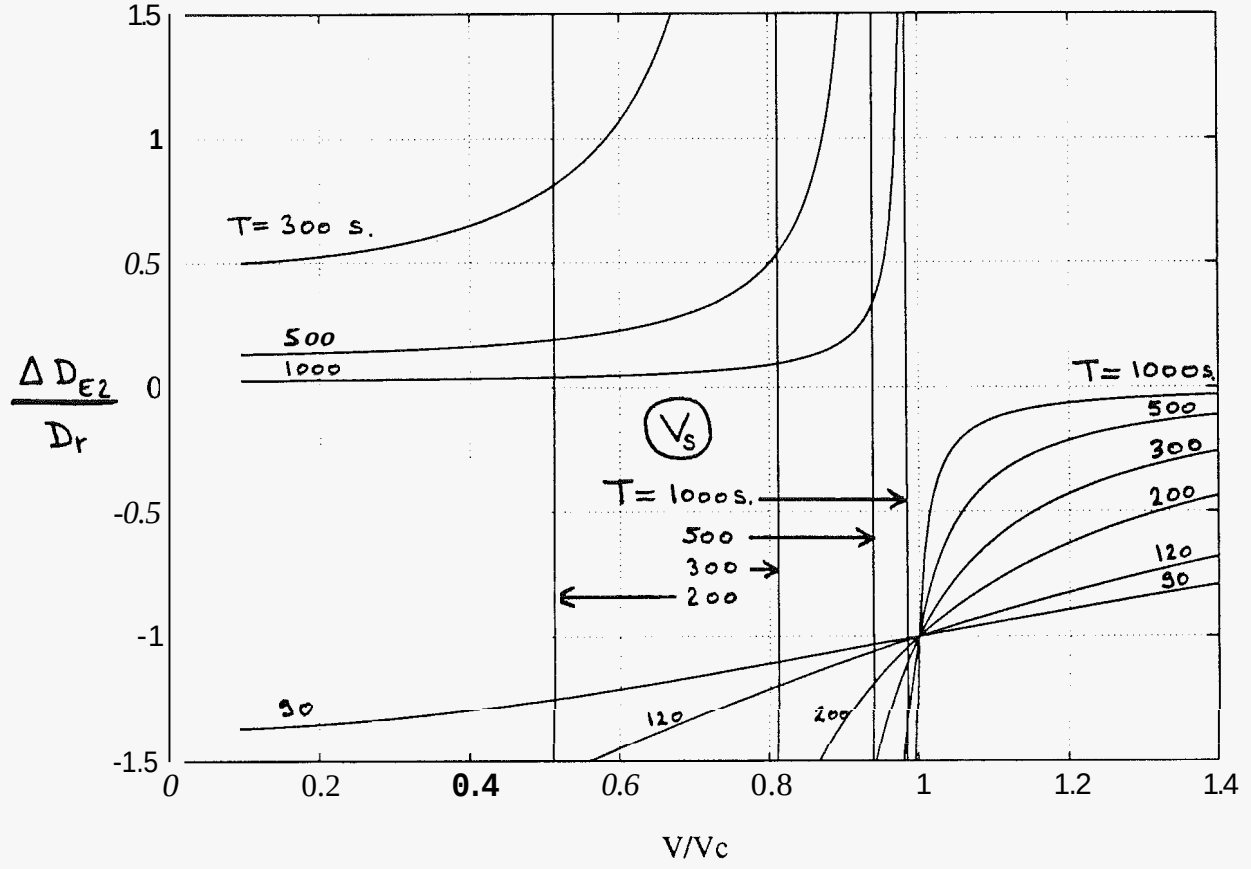

Fig. 4: Phase Portrait (T = 500 s Dr = 9 m/s2 V = 4->2.5 k d s)

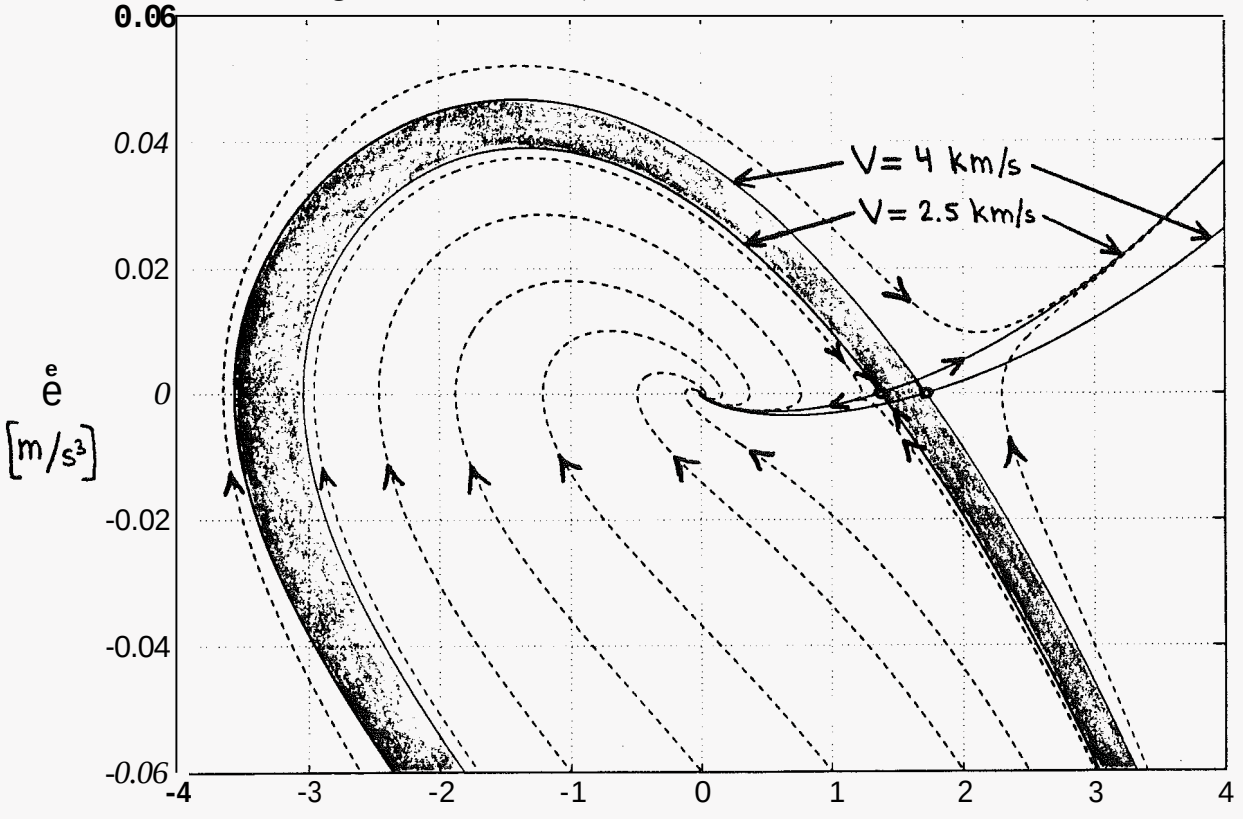

Fig. 5a: Basins of Attraction (V = **4** km/s Dr = 9 m/s2)

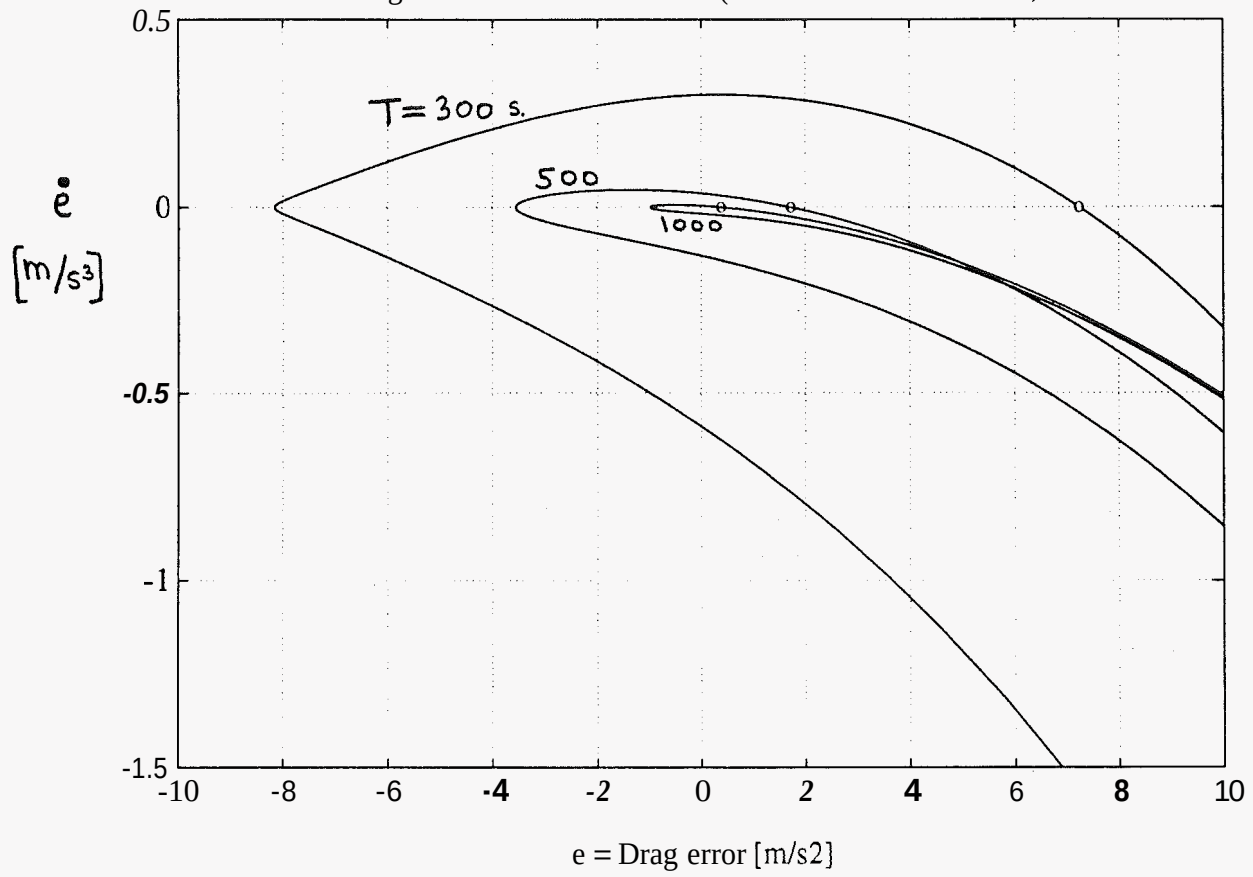

Fig. 5b: Basins of Attraction (V = 10 km/s Dr = **4** m/s2)

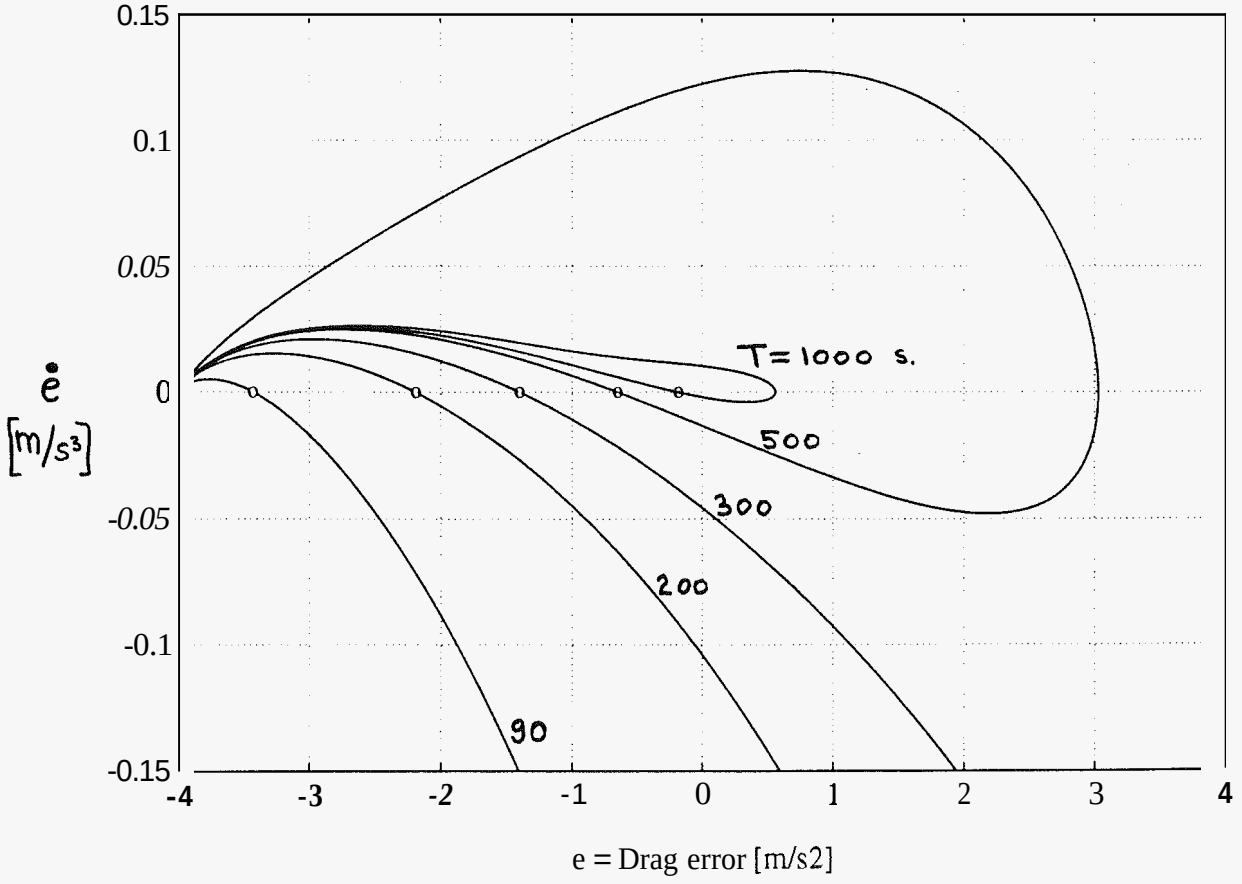

Fig. 6: Phase Portraits & Saturation Boundaries (T = 200 s Dr = 7 *d s 2* V = 7.8->5 km/s)

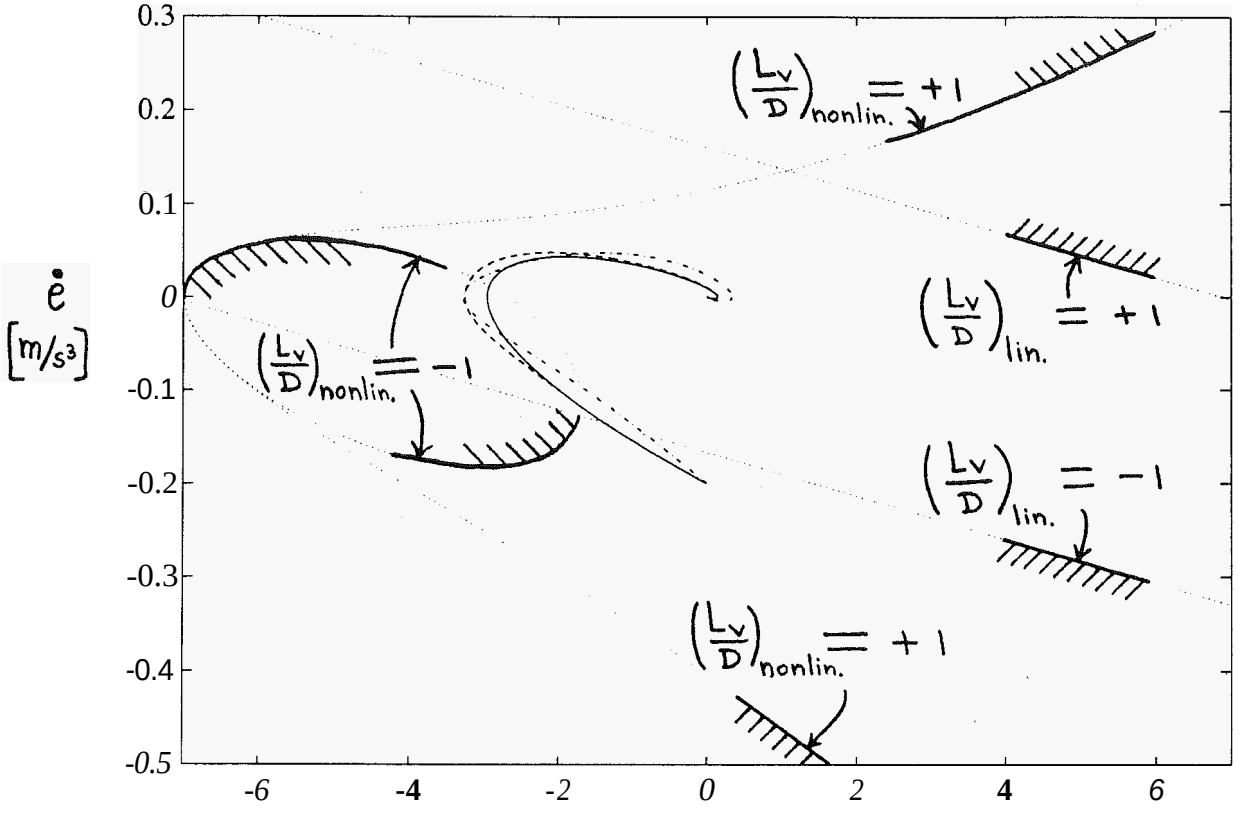

Fig. 7: Time Response (T = 200 s Dr = 7 m/s2 V = 7.8->5 km/s)